Sol-Gel-Derived Materials for Production of Pin-Printed Reporter Gene Living-Cell Microarrays

ARTICLE *in* ANALYTICAL CHEMISTRY · NOVEMBER 2013

Impact Factor: 5.64 · DOI: 10.1021/ac403220g · Source: PubMed

4 AUTHORS, INCLUDING:

Xin Ge
University of California, Riverside
15 PUBLICATIONS **333** CITATIONS
SEE PROFILE

Si Amar Dahoumane
Nano-Material Science, Biotechnology
17 PUBLICATIONS **233** CITATIONS
SEE PROFILE

analytical chemistry

Article

pubs.acs.org/ac

Sol–Gel-Derived Materials for Production of Pin-Printed Reporter Gene Living-Cell Microarrays

Xin Ge,*[,†,‡] Nikolas M. Eleftheriou,[†,§] Si Amar Dahoumane,[†] and John D. Brennan*[,†]

[†]Biointerfaces Institute and Department of Chemistry and Chemical Biology, McMaster University, Hamilton, ON, Canada L8S 4L8

[‡]Department of Chemical and Environmental Engineering, University of California, Riverside, CA 92521

[§]Department of Laboratory Medicine, Lund University, Lund, Sweden

ABSTRACT: We report the fabrication of three-dimensional living-cell microarrays via pin-printing of soft sol–gel-derived silica materials containing bacterial cells. Bacterial cells entrapped in the silica–glycerol microarray spots can express reporter genes and produce strong fluorescence signals. The signals responded to the presence and concentration of inducers or repressors as expected, indicating that the entrapped cells remained metabolically active. Microscopic imaging of individual microarray spots at different culture times suggests that the entrapped cells can grow and divide, phenomena further confirmed by experiments in bulk sol–gel materials that demonstrated the increases of entrapped cell density and fluorescence during incubation in culture media. The cell microarrays can also be printed into 96-well glass bottom microtiter plates in a multiplexed manner, and the fluorescence signals generated were able to quantitatively and selectively respond to the concentration of inducers, thus demonstrating the potential for multitarget biosensing and high-throughput/high-content cell-based screening. The signal levels of bacterial cells in silica were significantly higher than those in alginate arrays, presumably due to viability of the entrapped cells in silica sol–gels. Microarray stability assays proved that the entrapped cells retained their physiological activity after storage for four weeks. Given that a large number of fluorescent and luminescent protein-based cell assays have been developed, the reporter gene living-cell microarrays demonstrated in this paper are expected to be applicable to a wide variety of research areas ranging from bioanalysis and chemical biology to drug discovery and probing of cell–material interactions.

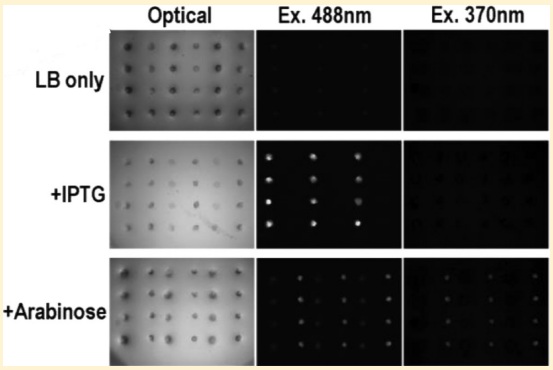

Cell-based assays play important roles in many applications such as whole-cell sensors,[1,2] and small-/biomacromolecule screening.[3−5] In genomics and proteomics studies, multiplexed approaches for globally analyzing cell phenotypes have greatly facilitated our understanding of cellular function. However, genome-wide assaying of cellular phenotypes is hindered by several challenges. For example, such large-scale analyses require that cells can be grown in parallel to synchronize cell cycle and be assayed in a miniaturized format in a manner that avoids cross-contamination between cell lines. Cells must also be present on a transparent support to allow spectroscopic analysis of phenotypes, usually by microscopic imaging or spectroscopy. In addition, the solid support must be durable and yet allow cell growth under a variety of growth conditions. Finally, the cells must be able to access the necessary nutrients, chemical compounds, and other reagents as well as exogenous molecules that might affect a particular biological process.[6]

Cell microarray techniques are emerging to address the problems outlined above.[7,8] A microarray is a highly parallelized miniaturized format allowing reduced cost, higher assay speed, and lower reagent consumption.[9,10] Several methods have been developed to produce cell-based microarrays, including: (1) using arrays of reagents, such as antibodies, cell-adhesive collagen I, film-deposited peptide-polymer, polymer-modified surfaces, and biocompatible anchors for membrane components to capture cells on the basis of the recognition of specific cell surface markers;[11−16] (2) transfection cell microarrays produced by growth of a layer of cells on an array of cDNA or RNAi that is immobilized in a hydrogel;[17] (3) the growth of cells within microchambers that are formed on permeable membranes;[6] and (4) entrapment of cells within alginate gels,[18−20] gelatin-based hydrogels,[21] or stretchable PDMS-derived microwell arrays,[22] and the culturing of the cells within silicon microarrays.[23] More recently, genetically engineered cells were able to be printed directly onto inert surfaces via overexpression of adhesive extra-cellular protein components.[24]

An emerging method for cell immobilization is their entrapment within sol–gel-derived silica materials.[25,26] Initial studies on the encapsulation of cells within sol–gel-derived media involved *Saccharomyces cerevisiae*.[27] Several bacterial strains,[28−31] plant and microalgae cells[32−34] as well as

Received: October 7, 2013
Accepted: November 21, 2013

   dx.doi.org/10.1021/ac403220g | *Anal. Chem.* XXXX, XXX, XXX–XXX

mammalian cells,[35] including pancreatic islets of Langerhans[36,37] and rat mature ovarian follicles,[38] have also been successfully immobilized in silica gels using both traditional sol−gel processing and aerosol-based methods.[39] The entrapped cells retain their ability to express fluorescent proteins[31,40] or to produce hormones or other species.[38] They can also be used as components of biosensors, for example, cell-based organophosphate biosensors have been reported.[41] In most cases, entrapped cells are unable to divide within the silica matrix.[25] However, multi-layered silica thin films have recently been utilized to entrap *E. coli* cells, which can survive, divide, and express fluorescent proteins in silica sol−gel materials.[42] In addition, *S. cerevisiae* cells have been encapsulated in poly(glycerol) silicate derived matrices, and the entrapped cells showed metabolic activity with long-term viability.[43]

Sol−gel-based materials have also been utilized for the fabrication of three-dimensional protein microarrays.[44−47] Such arrays have been utilized both for multiplexed biosensing, quantitative small molecule screening, and miniaturized cytotoxicity assays.[26] However, the use of sol−gel-based encapsulation for the preparation of high-density living cell microarrays has not been reported. The objective of this study was therefore to develop a method to entrap viable cells transformed with reporter genes into soft biocompatible sol−gel-derived nanocomposite silica materials that could retain cell growth and division, prevent them from leaching, and be pin-printed as microarrays. Such arrays result in cells that are located in individual array elements, and array formation can be done using both planar slides and microwell plates without the need for specially treated surfaces or adherent cell lines. These arrays provide a platform for rapidly screening multiple compounds against multiple targets in a single assay (i.e., many vs many screening). Other advantages of such arrays include: ease of integration into HTS facilities; minimal use of reagents; the potential for quantitative, multipoint screening; and the ability to store and transport the microarray after production to allow use in the field. Herein, we describe the fabrication and evaluation of 3D reporter gene bacterial cell microarrays and demonstrate their utility for fluorescence-based multiplexed cellular assays.

EXPERIMENTAL SECTION

Plasmids and Bacterial Stains. Reporter gene assays were done using *E. coli* for proof-of-concept studies on sol−gel-derived cell microarrays owing to the ease of transforming reporter genes into *E. coli* and the widespread use of *E. coli* as a model system for antimicrobial research. The expression of a reporter protein as a signaling method was based on the desire to have a signal that could both demonstrate cell viability upon entrapment and act as a quantitative signal for applications of cell arrays in sensing and screening. The plasmids utilized in this study were pGLO (Bio-Rad), which carries genes encoding for the arabinose operon regulation protein *araC*, and a green fluorescent protein (GFP) under the control of the arabinose promoter, and pET23a-eGFP (a gift from Dr. Gerry Wright), which uses the pET23a (Novagen) as the backbone, and encodes eGFP under the control of the T7 promoter. The GFP expressed by the pGLO plasmid is GFPuv, which has excitation maxima at 370 nm and 490 nm, while the GFP expressed by the pET23a plasmid is eGFP, having an excitation maximum at 490 nm. pGLO was transformed into *E. coli* HB101 using the standard $CaCl_2$ competent cell method. The pET23a−eGFP plasmid was transformed to BL21(DE3)pLys *E.coli* (Novagen). This host cell was chosen because it contains a plasmid encoding the T7 lysozyme gene, which lowers the background expression of the target gene, but does not interfere with the expression level following IPTG induction.

Preparation of Cells. From the fresh transformation plates, a single colony was picked and inoculated into LB medium with the addition of appropriate antibiotics: 100 μg/mL ampicillin for pGLO(HB101) and 100 μg/mL ampicillin and 34 μg/mL chloramphenicol for pET23a-eGFP(BL21,DE3,pLys). Cells were cultured at 37 °C to reach the late exponential phase, as indicated by an OD_{600} ∼0.8 (about 4×10^8 cells/mL). Cells were harvested by centrifugation and washed once with 0.85% NaCl. Typically, cells collected from 5 mL of culture media were resuspended into 100 μL of 0.85% NaCl, giving a cell density 50× as high as that in the culture media.

Preparation of Spotting Solutions. For fabrication of soft silica-based cell microarrays, 2.9 g of sodium silicate (SS, 27 wt % SiO_2, 10 wt % NaOH, Riedel-de Haën) was diluted with 10 mL of distilled, deionized water (Milli-Q Synthesis A10, Millipore, Inc., Billerica, MA), and mixed with 5 g of Dowex strong acid cation-exchange resin (Sigma, Oakville, ON). The mixture was immediately stirred for 30 s to lower the pH to a value of 4.0. The mixture was filtered through Whatman no. 1 filter paper and then through a 0.2 μm membrane syringe filter to remove the resin particles, resulting in a silicate solution containing 6 wt % SiO_2. The silica solution was mixed with an equal volume of 80% glycerol in water, and an appropriate amount of 1.0 N NaOH was added and immediately mixed to adjust the pH to 7.0, resulting in a glycerol−silicate solution (GSS). Solutions for microarraying were prepared by mixing a volume of 80 μL of GSS with 10 μL of HEPES buffer (0.5 M, pH 7.5) and 6−12 μL of the 50× cell suspension in a 96-well plate so that the final concentrations of the solution were 50 mM HEPES, 32% glycerol, 2.4% silica, pH 7.0, containing cells having 3 to 6× the density in the culture media (approximately equal to $1.2-2.4 \times 10^9$ cells/mL). Alginate-based cell microarray spotting solutions were prepared as described previously[18] with minor modifications. Briefly, 50× cell suspensions were mixed with 3% sodium alginate (Fluka) to give a spotting solution containing 1.5% sodium alginate, 24% glycerol, 50 mM HEPES (pH 7.5), and 10% (v/v) (5×) cell suspension. For gelatin microarrays, 2.0% gelatin (pork skin, Sigma) was prepared and melted by heating to 50 °C; it was then kept liquefied at 40 °C. The gelatin-based cell microarray spotting solution contained 1% gelatin and approximately 2×10^9 cells/mL. In the sodium silicate sol−gel solution supplemented with peptide detergent as the cell-stabilizing additive, the final concentrations were 2.4% SS, 50 mM HEPES (pH∼7), 0.1−0.4 mg/mL peptide acetyl-AAAAAAK (A6K, Sigma Genosys) or VVVVVVD (V6D, Sigma Genosys), and $\sim 2 \times 10^9$ cells/mL.

Microspotting and Cell Microarray Incubation. The silica and alginate spotting solutions containing the reporter gene cells were spotted using a Virtek Chipwriter contact pin-printer equipped with either a SMP3 stealth quill pin (0.7 nL delivery; 100 μm spot diameter) or a SMP7 quill pin (2.3 nL delivery; 235 μm spot diameter) (ArrayIt). Virtek Chipwriter Pro software was used to control all the parameters associated with microarraying, such as sample position, spot position and interelement spacing. Cell microarrays were printed into wells of 96-well glass-bottom microplates (Whatman, Cat. No. 7706−2370) without any surface pretreatment. Printing was

dx.doi.org/10.1021/ac403220g | *Anal. Chem.* XXXX, XXX, XXX−XXX

done at room temperature (21 ± 2 °C) at ~90% relative humidity to retard evaporation of water from the spots. Completion of an array of 100 spots (10 × 10) took about 2 min to perform, including pin wash cycles, when using a printhead speed of 16 mm.s^{-1}. After microspotting, silica-based cell arrays were aged inside the arrayer chamber for 30 min, then 100 μL of LB culture media (optionally supplemented with an appropriate inducer or repressor) was added into each microwell. For alginate-based cell arrays, arrays were aged for 5 min, then 100 mM $CaCl_2$ was added to solidify the alginate gel for 15 min. The gelled alginate cell arrays were then washed with 0.85% NaCl, and incubated in LB media which was supplemented with 100 mM $CaCl_2$ to keep the alginate in the solid form. To perform reporter gene assays, the cell arrays were incubated in culture media either at 37 °C for 3 h or at room temperature overnight (~14 h). The concentrations of supplemented inducers were usually 0.2−1.0 mM for IPTG, and 0.03−3.0 mM for arabinose.

Microarray Imaging and Data Processing. Culture medium was removed before imaging, and cell microarrays were washed with 0.85% NaCl to remove any cells that might have leached during incubation. Failure to perform the washing step resulted in low, but observable background fluorescence outside of the array element. Optical and fluorescent images of cell microarrays were obtained using an Olympus BX50 brightfield/fluorescence microscope equipped with a mercury lamp and a Roper Scientific Coolsnap Fx CCD camera. Excitation was performed at either 370 or 488 nm by inserting appropriate bandpass filters into the excitation path. Emission was collected through either 2× or 10× objective lenses. High-resolution confocal fluorescence microscopy images were obtained using a Leica TCS SP5 microscope equipped with a 488 nm laser and a 63× glycerol immersion lens. All array data were analyzed using Array-Pro Analyzer software. Processing typically consisted of integrating the intensity within a constant area in each array element (90% of full area), averaging the intensity over at least three identical array elements, and optionally normalizing the data. Background subtraction was not done.

Cell Division Studies. To study cell division within the sol−gel-derived materials, the biomaterials were prepared as described earlier (cf. the Preparation of Spotting Solutions section) with a cell density of 5×, but they were prepared as monolithic materials within microtiter plates. A volume of 100 μL of the biocomposite material was supplemented with 200 μL of minimal culture media (M9, 0.4% dextrose). An Infinite M1000 plate reader and the iControl software (TECAN, Männedorf, Switzerland) were used to measure absorbance and fluorescence initially and over time. Absorbance was collected at 600 nm. Fluorescence parameters were as follows: excitation 488 nm, bandwidth 5 nm; emission 510 nm, bandwidth 10 nm; bottom read. Temperature was set at 24 °C for all measurements. Assays were run in triplicate, and the background was subtracted.

RESULTS AND DISCUSSION

Material Selection. Five sol−gel materials were tested for their ability to fabricate microarrays with entrapped, living microbial cells. These materials were alginate with glycerol,[18−20] alginate with a sodium silicate shell, gelatin,[21] sodium silicate with glycerol, and sodium silicate with peptides that can dramatically stabilize cellular components.[48] The latter material was chosen since the presence of the peptides such as acetyl-AAAAAAK or VVVVVVD prior to drying has been shown to stabilize cellular components such as the photosystem-I complex for weeks in its dried form at room temperature, suggesting peptide detergents may effectively stabilize cells in the solid-state. After sol−gel solution preparation, pin-printing, washing, and overnight incubation with culture media as described in the Experimental Section, the cell microarrays prepared with these materials were evaluated on the basis of their printability criteria, including spot uniformity, tolerance to washing, cell activity, and so forth. Aging time and conditions were also optimized for promising material candidates. Because the entrapped cells tested here were *E. coli* BL21 (DE3) transformed with a plasmid encoding the GFPuv gene, after incubation in LB media supplemented with arabinose as the inducer, the microarrays containing metabolically active cells were expected to generate fluorescent signals. As shown in Figure 1, only alginate (Figure 1A) and SS with glycerol (Figure 1B) were able to produce microarrays compatible with active microbial cells. Gelatin cell microarrays resulted in serious leaching with loss of the integrity of spots (Figure 1C). SS with peptides can generate spots with good integrity after washing and overnight incubation, but no fluorescence was detected (Figure 1D), presumably due to cell lysis caused by the peptide detergents. Alginate with a sodium silicate overlay failed to generate immobilized spots, and the cells cannot be tracked (image not shown). Different durations of aging in a high humidity chamber were tested for SS−glycerol sol−gel-derived cell microarrays, and the results indicated that at least 20 min were required for this SS material with a high content of glycerol (~32%) to solidify and immobilize on the surface. In the following experiments, 30 min of aging time was applied for SS−glycerol sol−gel-derived materials to produce robust cell microarrays.

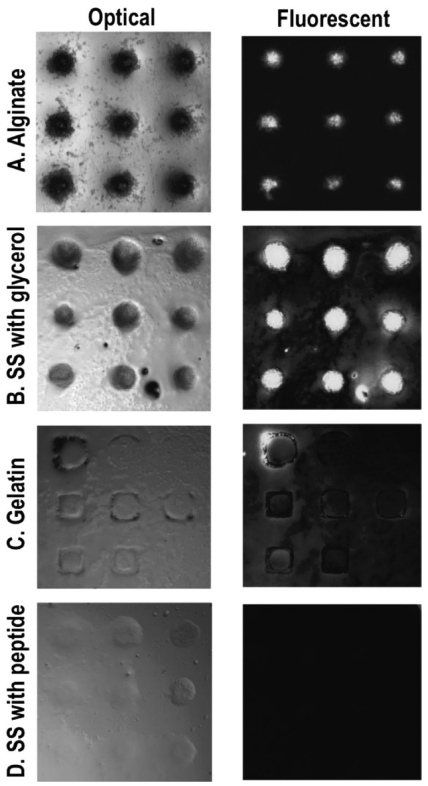

Figure 1. Sol−gel material selection for living-cell microarrays.

dx.doi.org/10.1021/ac403220g | *Anal. Chem.* XXXX, XXX, XXX−XXX

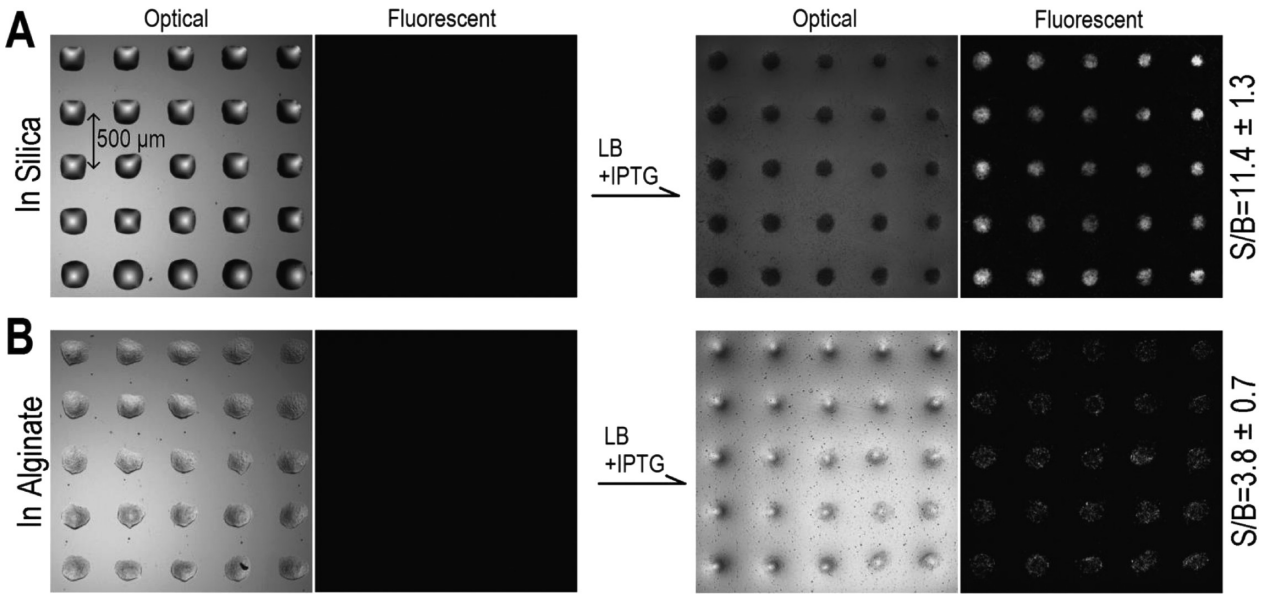

Figure 2. Viability of cell microarrays demonstrated by reporter gene expression. *E. coli* stain BL21 (DE3) pLys, carrying plasmid pET23a-eGFP, was immobilized in sol−gel-based silica (A) and alginate (B) materials. Both optical and fluorescent images of microarrays were taken before (left) and after (right) incubation in LB media supplemented with 1 mM IPTG. Signal-to-background ratios (S/B) are listed.

Optimizing Microarraying Conditions. Recent studies on the fabrication of protein microarrays by pin-printing of sol−gel-derived biocomposites have demonstrated that materials derived from sodium silicate or diglycerylsilane (DGS) and containing polymer additives such as poly(ethylene)glycol or poly(vinylalcohol) have long gelation times (a requirement for printing higher density arrays) and produce arrays that show good adhesion to a variety of surfaces, no cracking upon introduction of assay reagents, and high bioactivity for the entrapped biomolecules.[44,45] In the case of cell microarrays, we selected a sodium-silicate-derived material with an intermediate silica density (2.4 wt % silica) and a relatively high level of glycerol (32% v/v) and performed printing at neutral pH (7.0) to ensure long gelation times (>1 h) and to reduce the effects of dehydration, allowing for longer cure times and thus greater syneresis, and incubated the arrays at a high relative humidity (~90% RH) to retard the evaporation of water from the spots. This material could be cured for as little as 30 min after printing and prior to addition of media, which was sufficient to retain cell viability and yet avoid substantial leaching of cells. It is worthwhile to mention that the degree of cell leaching is indeed dependent on initial cell density and growth rate. Less inoculation with suboptimal culture conditions, such as low temperature, usually results in less cell leaching. The material could be produced and arrayed with a variable density of cells, generally spanning from 0.1 to 10× of the density in the original culture medium, allowing for adjustment of the number of cells per array element. In this study, microarray spotting solutions typically had cell densities of 3 to 6× relative to the culture medium, approximately equal to $1-2 \times 10^9$ cells/mL, which was sufficient to produce high signal-to-background (S/B) ratios in subsequent assays.

Comparison of Silica and Alginate Cell Microarrays. A 5 × 5 microarray was printed into a single well of a glass bottom 96-well microplate to produce spots of 235 μm diameter with interspot spacings of 500 μm. After aging, the cell array was investigated by optical and fluorescent microscopic imaging. Figure 2A (left panel) shows that the microspots were uniform in size and shape and there was no detectable fluorescence because no inducer (IPTG) was added to the cell culture media. Another cell array was prepared in the same manner and then incubated in media containing 1 mM IPTG to induce the expression of a reporter gene, eGFP. The optical image of the cell array (Figure 2A (right panel)) showed that the silica spots were in good condition after incubation and that no material cracking was observed. The corresponding fluorescence image clearly demonstrates that the microarray was highly fluorescent after induction, providing direct evidence that the cells, immobilized in the microarray through entrapment in sol−gel-derived silica, were metabolically active and responsive to the presence of the inducer. In addition, the fluorescence signal was contained only within the microarray elements and was not detectable in the surrounding regions, which indicates that the cells did not leach significantly from the silicate gel during incubation and assaying. Quantitative analysis of the fluorescence signals revealed a high signal-to-background ratio with a small standard deviation (i.e., S/B is equal to 11.4 ± 1.3). The relative error of ~10% likely reflects the variation of array element sizes, which can be seen to slightly decrease going from left to right.

As a comparison, alginate-based cell microarrays, containing the same cell type at the same density, were prepared according to a previous report with minor modification.[18] The cell arrays were then incubated in LB media with or without addition of IPTG. It is important to note that 100 mM $CaCl_2$ was required to solidify the alginate gel, and thus it was added into the culture media to keep the alginate gelled. After incubation, optical and fluorescence images of alginate cell microarrays were obtained and are shown in Figure 2B. Consistent with the cell microarrays made of silica material, the alginate arrays can be printed uniformly, and there was no background fluorescence prior to addition of inducer (left panel). Upon addition of inducer, fluorescence signals were generated in the alginate cell arrays (right panel). However, the signal level was significantly lower than that obtained in the silica-based cell microarrays. Quantitative analysis revealed that the S/B was

dx.doi.org/10.1021/ac403220g | *Anal. Chem.* XXXX, XXX, XXX−XXX

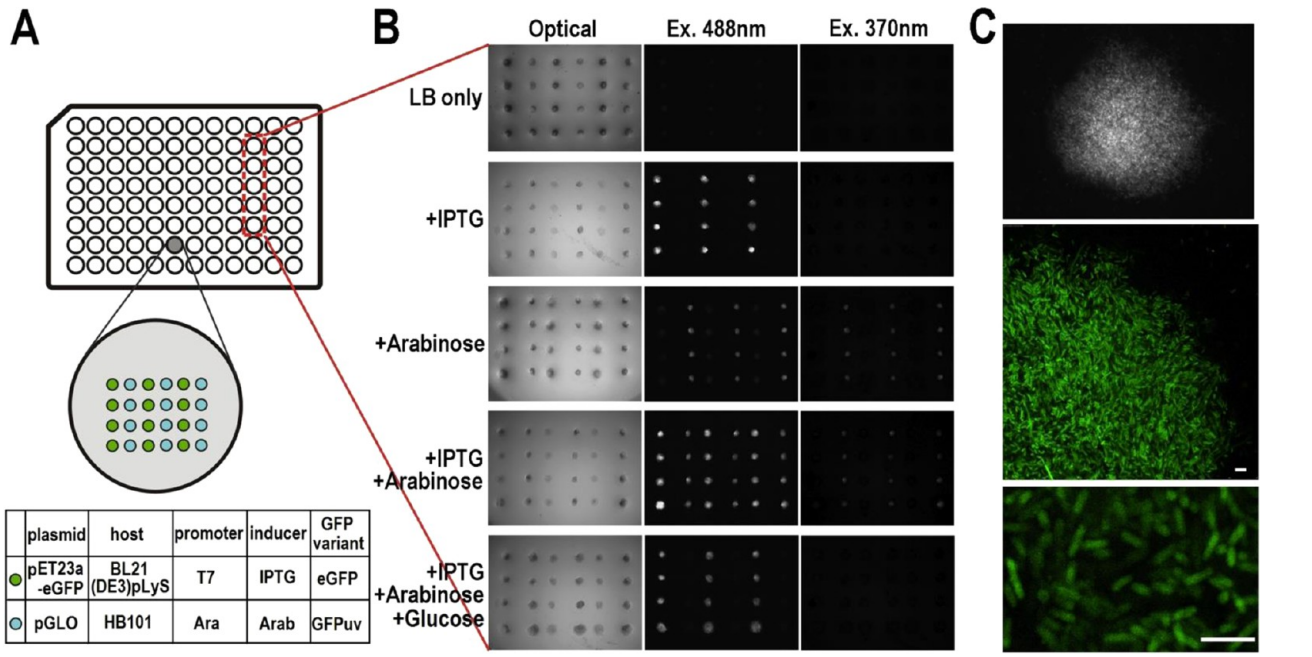

Figure 3. Multiplexed assays using cell microarrays. (A) Supergridded cell microarrays were printed into a 96-well plate (top). In each single well, two strains were pin-printed in alternate columns (middle). Information on the two *E. coli* strains, for example, plasmid, host cell, promoter, inducer, and GFP variant is shown in the Table (bottom). (B) Microscopic images of five-cell microarrays pin-printed separately in wells and incubated in different culture media (LB only; with addition of IPTG; arabinose; IPTG and arabinose; IPTG, arabinose, and glucose). Three images were taken for each cell array—an optical image, a fluorescence image excited at 488 nm, and a fluorescence image excited at 370 nm. (C) Confocal microscopic images of an individual microspot in the array with increased magnification. Scale bars are 5 μm.

equal to 3.8 ± 0.7, which is 3-fold less than the S/B ratio of the silica-based microarrays.

In addition to the lower signal-to-background ratio, two other disadvantages were also associated with alginate-based cell microarrays: (1) Ca^{2+} or other bivalent metal ions must be present, which limits its applications in pathway studies involving Ca^{2+}, and (2) although alginate is an attractive material due to its biocompatibility and ability to form hydrogels, its slow and uncontrollable degradation can be an undesirable feature.[49] Degradation diminishes the long-term storage stability of these cell microarrays and limits their usage for organisms that digest such polysaccharides. Although a few studies suggest that entrapment in silica can induce stress-response genes or regulate induction or repression of a limited number of genes,[50] the effects of silica entrapment on *E. coli* transcriptomics has not been extensively characterized. Further investigation across a range of various *E. coli* promoters can address this issue and will be reported in a future study.

Overall, the studies described above prove that the use of a relatively soft silica-based sol with high glycerol content is suitable for fabrication of viable bacterial cell microarrays. The entrapped cells were metabolically active and responsive to the presence of inducer. The fluorescence signals were strong with good reproducibility. Furthermore, the ability to form the microarrays within the wells of microplates makes incubation and washing steps facile and also makes it amenable to integration with automated liquid handling, making the cell microarray technique described here readily adopted for HTS applications.

Multiplexed Sensing Using Reporter Gene Cell Microarrays. To demonstrate the ability to perform multiplexed assays using the silica-based cell microarray, two *E. coli* strains transformed with different plasmids were utilized to form microarrays. In addition to the BL21(DE3)pLys strain transformed with plasmid pET23a-eGFP used above, we also transformed the HB101 strain with plasmid pGLO, which carries genes encoding for the arabinose operon regulation protein *araC*, and a green fluorescent protein following the P_{BAD} promoter. The GFP in pGLO was the GFPuv mutant, which has an excitation maximum at 370 nm. Thus, discrimination of the two cell lines on the microarray can be done both on the basis of position and excitation wavelength. Another feature of the pGLO cells is that the expression of GFPuv can be induced by arabinose but is metabolically repressed by the presence of glucose.[51,52] Further information on these two strains, including host cells, plasmids, promoters, inducers, and report genes are listed in Figure 3A.

Microarrays (6 × 4) containing alternating columns of the two *E. coli* strains were pin-printed into five separate wells of a microplate, in the pattern illustrated in Figure 3A. Microarrays were incubated in five different culture media, each supplemented with a different inducer or repressor. After incubation, images of the arrays were taken in three channels: optical, fluorescence excited at 488 nm and at 370 nm. Optical images show the location of all microspots, and fluorescent images show reporter gene expression in the cell arrays (Figure 3B). For the array incubated in LB medium without any inducer (row 1 in Figure 3B), weak fluorescent signals (S/B = 1.8 ± 0.3) were generated in the microspots containing BL21(DE3)pLys (pET23a-eGFP), due to the leaky expression of the T7 promoter. Microspots containing cells carrying the P_{BAD} promoter had no detectable fluorescence, since the *Ara* operon gives tightly controlled transcription and thus very low basal expression.[51] When IPTG was added to the LB medium to a final concentration of 0.2 mM (row 2), only the microspots having the T7 promoter produced fluorescence signals (S/B =

dx.doi.org/10.1021/ac403220g | *Anal. Chem.* XXXX, XXX, XXX–XXX

10.6 ± 1.7), while microspots containing HB101 (pGLO) remained nonfluorescent. The relative errors for arrays formed in microwells (15−20%) were generally higher than those formed on glass slides (~10%) owing to a larger variation in spot sizes, as seen in Figure 3B. When the array was cultured in LB with 3 mM arabinose (row 3), it gave a result opposite to that of LB+IPTG (row 2): the microspots having arabinose promoter were highly fluorescent (S/B = 7.4 ± 1.2), while microspots containing the T7 promoter remained at the background signal level (S/B = 2.3 ± 0.4). The lower signal level is due to the lower emissivity of the GFPUv relative to eGFP. With addition of both inducers (row 4), the whole cell microarray had strong fluorescence, with T7 containing cells having an S/B of 11.7 ± 2.0 and P_{BAD} cells having an S/B of 7.3 ± 1.5. These numbers were in good agreement with the S/B values obtained in rows 2 and 3 in Figure 3B. In the fifth well, the cell microarray was incubated in LB supplemented with two inducers and one repressor—0.2 mM IPTG, 3 mM arabinose, and 1% glucose. The result showed that microspots having a T7 promoter produced fluorescence with an S/B equal to 8.4 ± 1.3, slightly less than the data of arrays incubated in ITPG−glucose LB media (row 2 and 4), while microspots containing HB101 (pGLO) had no detectable fluorescence, reflecting the fact that the *Ara* operon was repressed by the presence of glucose.[51] The lower value for the T7 promoter in the presence of glucose is due to the ability of glucose to repress the basal expression caused by T7 leakage but not interfere with the expression level following IPTG induction.[53]

To selectively excite the GFPuv mutant encoded by pGLO, the microarray was excited at 370 nm. Under these conditions, the HB101 (pGLO) microspots showed a fluorescence signal of 4.9 ± 0.8, while microspots containing the T7 system showed no detectable fluorescence. Thus, it is possible to enhance selectivity in array-based reporter gene assays via selection of the excitation wavelength. All of the above results demonstrate that cell strains, which carry two GFP variants under the control of different promoter systems, are viable and respond selectively to the presence of inducers or repressors as expected. The ability to perform multiplexed assays using three-dimensional cell microarrays provides an important resource for both multianalyte sensing and as a tool for rapid, "many vs many" small molecule screening—a task that is not easy to implement in current HTS facilities.

Figure 3C shows high magnification fluorescent images of the cell microarray. The image of an individual microspot (Figure 3C, top) indicates that it has a clear edge, suggesting that the cells remain entrapped within the gel and thus should show a low level of cross-contamination. A higher magnification image of a microspot (Figure 3C, middle) reveals that the cells are present in the microspots at a very high density, which is likely the reason why these arrays can achieve a high S/B ratio. A close-up image (Figure 3C, bottom) shows individual entrapped *E. coli* cells, which are fluorescent, proving that the signals were indeed generated by the expression of GFP in intact, living cells.

Cell Division in Microspots. The images shown in Figure 3C reveal high cell densities within microspots, which may help explain the S/B difference between alginate and silicate materials (described in Figure 2). Both alginate and silica microspots contained identical numbers of cells prior to incubation and induction. However, the final signal for silica spots was almost 3-fold higher than in alginate. High magnification fluorescence images of silica and alginate arrays after induction showed a much higher cell density in the silica gel (compare Figures 2B and 3C). Given that the same number of cells were introduced to the two materials, the increased number of fluorescent cells suggests that the silica either has a much higher fraction of viable cells, a higher level of GFP induction per cell, or that the cells entrapped in silica gel with a high glycerol content may still have the ability to divide. To distinguish between these possibilities, two different cell arrays were printed. In the first array, the HB101 (pGLO) cells were first induced in LB media supplemented with arabinose, followed by pin-printed and imaging to provide a baseline fluorescence signal from induced cells at a set cell concentration. Microscopic fluorescent images show approximately 200 cells were entrapped per microspot (Figure 4, left),

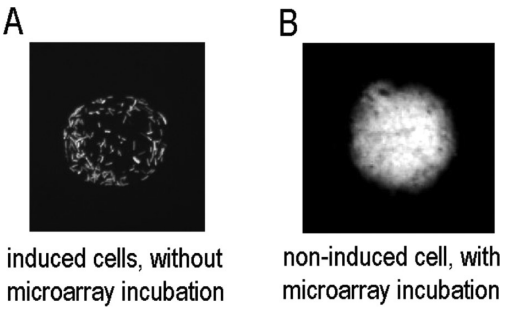

Figure 4. Cell growth in silica gel with high glycerol content. (A) Fluorescence image of a microspot containing cells induced prior to printing. Induced cells were prepared by culturing HB101 (pGLO) in LB with addition of arabinose to OD_{600} = 1.0. Cell suspension was mixed with silicate precursor to make the spotting solution containing cells at a density 5× relative to the OD = 1.0 media. (B) Fluorescent image of a microspot after incubation in LB supplemented with 3 mM arabinose media. Cells were prepared by culturing HB101 (pGLO) in LB without addition of inducer to OD_{600} = 1.0. Spotting solutions containing noninduced cells had the same cell density (5 ×) as that used in (A).

a number consistent with expectations giving the OD of cells present in the volume of a pin-printed spot. In the second array, noninduced cells (cultured in LB only) were printed at the same cell density as in the first array and then incubated with LB + arabinose. The microscopic fluorescent images (Figure 4, right) show that the intensity is significantly higher after incubation with a significantly increased number of visible cells, suggesting cells can grow and divide in the low density, soft sol−gel-based material. It is important to notice that even if the cell division occurred within this material, the array spots remained on the glass slide without any shift of location or loss of integrity, as confirmed by optical and fluorescent microscopic imaging.

To further evaluate cell division, we also performed a separate study using an identical material formed as a monolith (~3 mm thickness) in a 96-microwell plate seeded with noninduced cells. It allowed observation of both OD_{600} and fluorescence intensity changes over the culture time, which would be difficult to perform on a microarray. As shown in Figure 5, entrapped cells showed a clear increase in both OD_{600} and fluorescence intensity, with both signals reaching their plateaus. Buffer exchanges were performed at the end of the growth period, and media were measured with OD_{600}. The results indicated that cell leaching was less than 10%, confirming that the growth curves were related to entrapped cells. It is important to note that previous reports suggest that

dx.doi.org/10.1021/ac403220g | *Anal. Chem.* XXXX, XXX, XXX−XXX

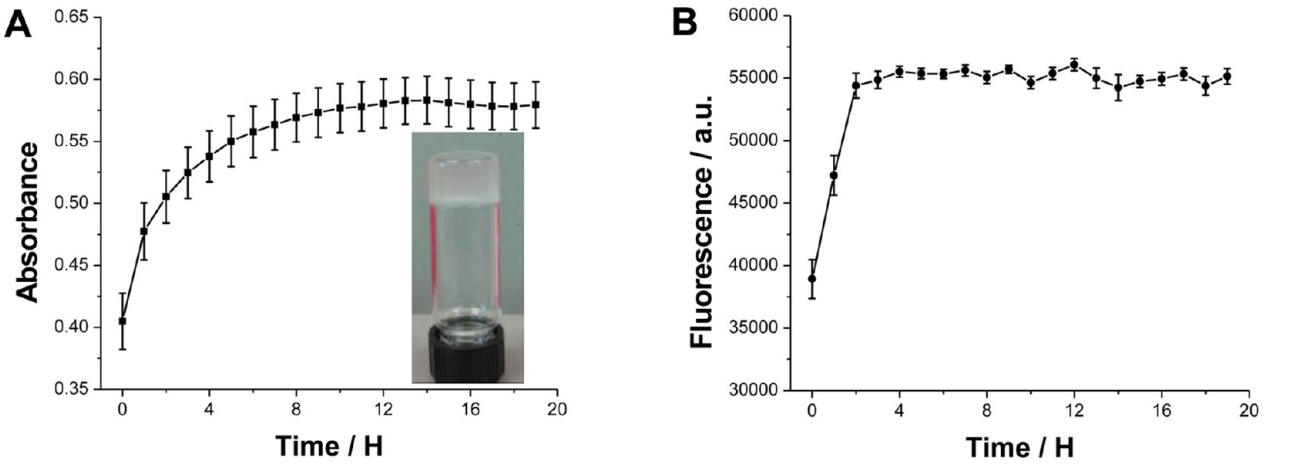

Figure 5. Entrapped cells are viable and allow determination of biological function in monolithic silica gels supplemented with 32% glycerol. (A) OD_{600} growth curve of *E. coli* HB101 (transformed with pGLO) in a monolith and (inset) picture of a sol–gel monolith made of the same material with the same density of cells. (B) Fluorescence signals of HB101 (pGLO) culture in a monolith.

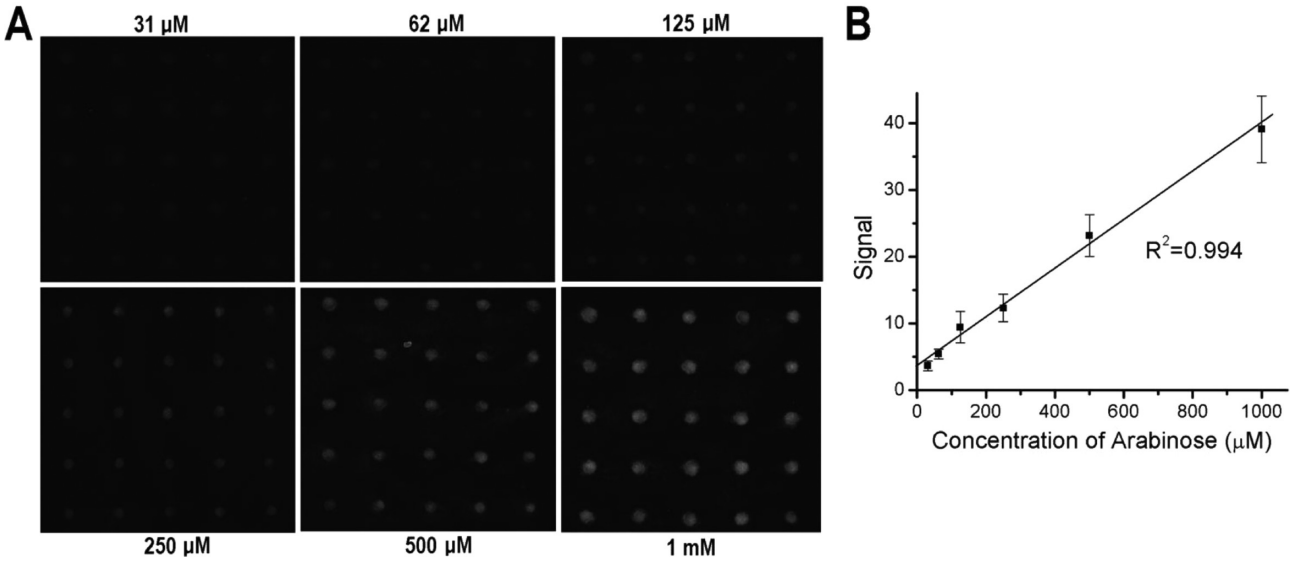

Figure 6. Fluorescence images of *E. coli* HB101 (pGLO) arrays, after incubation in LB with addition of arabinose at a series of concentrations, from 31 μM to 1 mM. (B) Signal vs arabinose concentration. Note that background signals were not subtracted (background fluorescence was undetectable).

cells do not divide when encapsulated in silica gels, either with or without glycerol at low concentrations (10% v/v),[31,54] but the behavior of entrapped *E. coli* cells has been explored further in a related study,[55] which also showed division of cells in soft silica materials and <10% leaching. In this study, 32% (v/v) glycerol was used for sol–gel preparation, and the results suggest that this condition can retain the viability of entrapped cells. Presumably, the viability of cells entrapped in the silica matrix is attributed to the high concentration of glycerol, an observation which is consistent to the results of encapsulation of yeast cells utilizing poly(glycerol)-silicate-derived soft matrices.[48] The ability to sustain cell growth within the sol–gel-derived material is believed to be extremely valuable to allow screening for bacteriostatic agents, as loss of cell division pathways would make identification of antimicrobial action difficult to assess. In addition, cell growth can support long-term and more complicated cellular responses (e.g., signal transduction and specific gene expression). Further studies on cell division within various sol–gel-derived materials as monoliths or at the microscale level are needed to better understand the relationship between cell division and the mechanical properties of the materials.

Quantitative Sensing. For biosensing applications, it is essential to obtain quantitative data that reflect the amount of analyte presented in a sample. It is known that gene expression from the *araBAD* promoter can be modulated over several orders of magnitude by the concentration of arabinose in the growth medium.[52] To demonstrate that the reporter gene cell microarrays described herein could generate quantitative signals, microarrays containing HB101 (pGLO) were prepared in individual microwells and exposed to media having a gradient of arabinose concentrations. After incubation, fluorescent images were taken, and the fluorescence signals were averaged over 25 microarray elements. The results, shown in Figure 6, indicate that the cell microarrays produced a linear response to arabinose concentration over the range from 31 μM to 1 mM. These results suggest that the silica-based cell microarray can be used for quantitative, reporter-gene-based biosensing in a

dx.doi.org/10.1021/ac403220g | *Anal. Chem.* XXXX, XXX, XXX–XXX

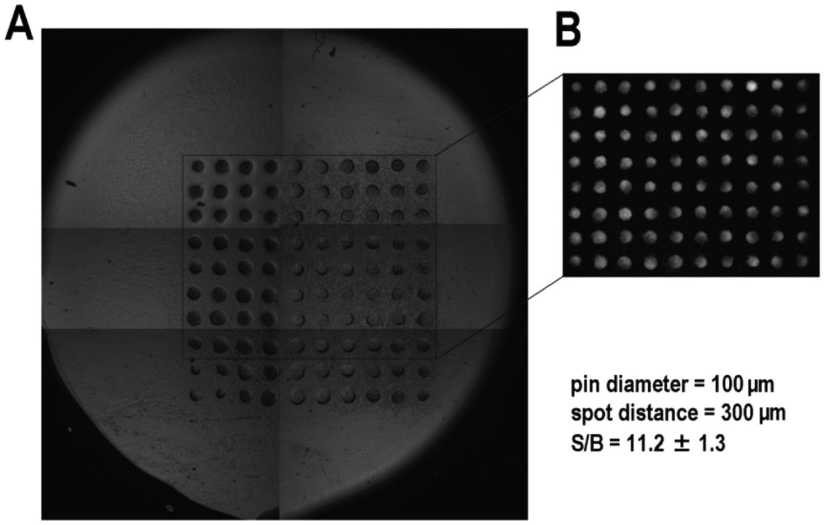

Figure 7. High density cell microarray in which (A) 100 spots were arrayed in a single microwell (diameter ~0.6 cm). Array elements have a diameter of 100 μm, while the distance between the centers of the adjacent spots was 300 μm. (B) Fluorescent image of the array.

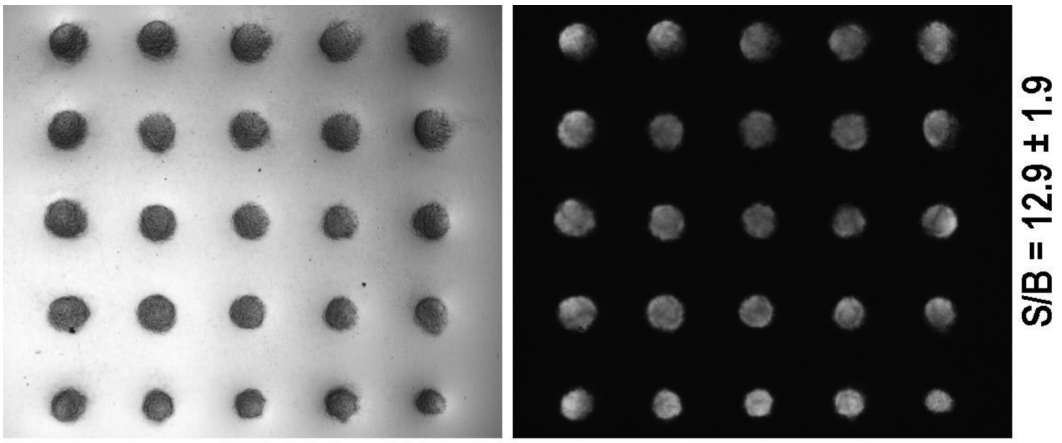

Figure 8. Storage stability of silica-gel-based cell microarrays. BL21(DE3)pLys cells carrying pET23a-eGFP were entrapped in pin-printed microarrays through the silicate sol–gel process. After 4 weeks of storage in LB media at 4 °C, the cell microarray was incubated with LB+IPTG media, and optical (left) and fluorescent (right) images were taken. The signal-to-background ratio (S/B) is shown to the right.

multiplexed manner and should also be amenable to quantitative high-throughput screening, where information on inhibitory concentrations is desired (e.g., minimum inhibitory concentrations or IC_{50} values).

High Density Cell Microarrays. All arrays described above utilized array elements of 235 μm diameter with 500 μm spacing, which limits the arrays to a total of ~40 elements per well of 96-well microplates. To increase array density, a Stealth SMP3 quill pin (with liquid delivery volume of ~0.7 nL) was used; this allows a smaller diameter microspot (≈100 μm) and closer interelement spacings (300 μm). Cell arrays contained BL21 DE3 pLys (pET23a–eGFP) and were printed and incubated in LB +IPTG media. The images of a 10 × 10 cell microarray are shown in Figure 7. The results show that the cells were active in the 100 μm microspots, and quantitative analysis reveals that the S/B ratio is equal to 11.2 ± 1.3, which is similar to that obtained using 235 μm spots (11.4 ± 1.3, Figure 2A). At this density, each well allows at least 100 cell-based assays to be done using as little as 40 μL of solution (minimum volume for 96-well plate assays), or 400 nL per assay. Alternatively, a library carrying the entire *E. coli* genome (~2000 promoters) could be printed in duplicate into only 40 wells, enabling genome-wide small molecule screening in ultrahigh-throughput. Assuming that 200 plates could be tested per day, this enables almost 2 million assays per day, which is beyond the current capacity of even the highest density, 3456-well plates.

Storage Stability. The storage stability of the cell microarrays was tested over a period of up to 4 weeks for arrays that were immersing in sterilized LB media at 4 °C. Microscopic observation showed that the silica spots were in good condition after storage, with no significant spot cracking or cell leaching. Following storage, the arrays were incubated in LB+IPTG media at 37 °C for 3 h. Quantitative analysis of the fluorescent images (Figure 8) indicated a high signal-to-background ratio, 12.9 ± 1.9, which was not statistically different from the signals obtained for fresh arrays (11.4 ± 1.3, Figure 2A). Previous studies have demonstrated that bacterial cells remained viable for 3 months when entrapped in monolithic silica gels.[54] Furthermore, given that the cell microarrays fabricated in the current study allow cell division and growth, the microarrays will maintain their biological function even if only a small fraction of cells per spot remain viable. Therefore, the cell microarrays described herein are

dx.doi.org/10.1021/ac403220g | *Anal. Chem.* XXXX, XXX, XXX–XXX

expected to have a good shelf life, which allows transporting to end users or remote sites for analysis in the field.

CONCLUSIONS

This manuscript describes a simple method to fabricate versatile, three-dimensional reporter gene cell microarrays using contact pin-printing of low density sol–gel-derived silica. Expression of reporter genes demonstrates that bacterial cells remain viable and biologically functional when entrapped in silica materials containing high levels of glycerol (32%). The cell-containing silica microspots can withstand prolonged incubation in complex culture media without cracking or severe cell leaching. High signal levels were achieved (i.e., the S/B ratio was usually >10) which was 3 times higher than the value obtained from alginate-based cell arrays. The ability for multiplexed assays was demonstrated using microarrays containing two stains carrying different reporter genes under the control of different promoter systems. The results showed that the arrays selectively responded to the presence of inducers and repressors, suggesting that the cell microarray has the potential for multiplexed HTS in a "many vs. many" format. The use of cell microarrays for quantitative analysis was also demonstrated. Finally, the cell microarrays were shown to remain stable for at least four weeks when stored in media, which may enable the use of such arrays for multiplexed sensing in the field. Further work remains to be done to fully evaluate and optimize the signaling and stability of these arrays. In addition, further studies are needed to expand the types of cells used for microarray fabrication, extend the types of reporter genes and promoters used, and further explore the use of such arrays for sensing and screening applications. The results of these studies will be reported in future manuscripts.

AUTHOR INFORMATION

Corresponding Authors

*E-mail: brennanj@mcmaster.ca (J.D.B.). Tel.: (905) 525-9140, ext. 20682. Internet: brennanlab.mcmaster.ca.

*E-mail: xge@engr.ucr.edu (X.G.). Tel.: (951) 827-6229. Internet: engr.ucr.edu/gelab.

Notes

The authors declare no competing financial interest.

ACKNOWLEDGMENTS

The authors thank the Ontario Centers of Excellence, the Natural Sciences and Engineering Research Council of Canada (NSERC) for provision of a Discovery Grant and a CREATE Biointerfaces Training Grant, the Canada Foundation for Innovation (CFI), and the Ontario Ministry of Research and Innovation for support of this work. J.D.B. holds the Canada Research Chair in Bioanalytical Chemistry and Biointerfaces.

REFERENCES

(1) Sorensen, S. J.; Burmolle, M.; Hansen, L. H. *Curr. Opin. Biotechnol.* **2006**, *17*, 11.
(2) Yagi, K. *Appl. Microbiol. Biotechnol.* **2007**, *73*, 1251.
(3) Johnston, P. A. *Drug Discovery Today* **2002**, *7*, 353.
(4) Gonzalez-Nicolini, V.; Fussenegger, M. *Anti-Cancer Drugs* **2005**, *16*, 223.
(5) Fan, F.; Wood, K. V. *Assay Drug Dev. Technol.* **2007**, *5*, 127.
(6) Xu, C. W. *Genome Res.* **2002**, *12*, 482.
(7) Papp, K.; Szittner, Z.; Prechl, J. *Cell. Mol. Life Sci.* **2012**, *69*, 2717.
(8) Al-Khaldi, S. F.; Mossoba, M. M.; Burke, T. L.; Fry, F. S. *Foodborne Pathog. Dis.* **2009**, *6*, 1001.
(9) Angres, B. *Exp. Rev. Molec. Diag.* **2005**, *5*, 769.
(10) Diaz-Mochon, J. J.; Tourniaire, G.; Bradley, M. *Chem. Soc. Rev.* **2007**, *36*, 449.
(11) Stone, J. D.; Demkowicz, W. E.; Stern, L. J. *Proc. Natl. Acad. Sci. U.S.A.* **2005**, *102*, 3744.
(12) Lee, J. Y.; Shah, S. S.; Yan, J.; Howland, M. C.; Parikh, A. N.; Pan, T.; Revzin, A. *Langmuir* **2009**, *25*, 3880.
(13) Petersen, S.; Loschonsky, S.; Prucker, O.; Ruhe, J.; Biesalski, M. *Phys. Status Solidi A* **2009**, *206*, 468.
(14) Mei, Y.; Hollister-Lock, J.; Bogatyrev, S. R.; Seung-Woo, C.; Weir, G. C.; Langer, R.; Anderson, D. G. *Biomaterials* **2010**, *31*, 8989.
(15) Kato, K.; Umezawa, K.; Funeriu, D. P.; Miyake, M.; Miyake, J.; Nagamune, T. *Biotechniques* **2003**, *35*, 1014.
(16) Kato, K.; Umezawa, K.; Miyake, M.; Miyake, J.; Nagamune, T. *Biotechniques* **2004**, *37*, 444.
(17) Ziauddin, J.; Sabatini, D. M. *Nature* **2001**, *411*, 107.
(18) Fesenko, D. O.; Nasedkina, T. V.; Chudinov, A. V.; Prokopenko, D. V.; Yurasov, R. A.; Zasedatelev, A. S. *Mol. Biol.* **2005**, *39*, 84.
(19) Fesenko, D. O.; Nasedkina, T. V.; Prokopenko, D. V.; Mirzabekov, A. D. *Biosens. Bioelectron.* **2005**, *20*, 1860.
(20) Fernandes, T. G.; Kwon, S.-J.; Lee, M.-Y.; Clark, D. S.; Cabral, J. M. S.; Dordick, J. S. *Anal. Chem.* **2008**, *17*, 6633–6639.
(21) Fu, Y.; Xu, K. D.; Zheng, X. X.; Giacomin, A. J.; Mix, A. W.; Kao, W. Y. J. *Biomaterials* **2012**, *33*, 48.
(22) Wang, Y. L.; Shah, P.; Phillips, C.; Sims, C. E.; Allbritton, N. L. *Anal. Bioanal. Chem.* **2012**, *402*, 1065.
(23) Nikkhah, M.; Strobl, J. S.; Schmelz, E. M.; Roberts, P. C.; Zhou, H.; Agah, M. *Biomaterials* **2011**, *32*, 7625.
(24) Melamed, S.; Ceriotti, L.; Weigel, W.; Rossi, F.; Colpo, P.; Belkin, S. *Lab Chip* **2011**, *11*, 139.
(25) Avnir, D.; Coradin, T.; Lev, O.; Livage, J. *J. Mater. Chem.* **2006**, *16*, 1013.
(26) Monton, M. R. N.; Forsberg, E. M.; Brennan, J. D. *Chem. Mater.* **2012**, *24*, 796.
(27) Inama, L.; Dire, S.; Carturan, G.; Cavazza, A. *J. Biotechnol.* **1993**, *30*, 197.
(28) RiettiShati, M.; Ronen, D.; Mandelbaum, R. T. *J. Sol–Gel Sci. Technol.* **1996**, *7*, 77.
(29) Nassif, N.; Bouvet, O.; Rager, M. N.; Roux, C.; Coradin, T.; Livage, J. *Nat. Mater.* **2002**, *1*, 42.
(30) Premkumar, J. R.; Lev, O.; Rosen, R.; Belkin, S. *Adv. Mater.* **2001**, *13*, 1773.
(31) Premkumar, J. R.; Sagi, E.; Rozen, R.; Belkin, S.; Modestov, A. D.; Lev, O. *Chem. Mater.* **2002**, *14*, 2676.
(32) Pressi, G.; Dal Toso, R.; Dal Monte, R.; Carturan, G. *J. Sol–Gel Sci. Technol.* **2003**, *26*, 1189.
(33) Sicard, C.; Brayner, R.; Margueritat, J.; Hemadi, M.; Coute, A.; Yepremian, C.; Djediat, C.; Aubard, J.; Fievet, F.; Livage, J.; Coradin, T. *J. Mater. Chem.* **2010**, *20*, 9342.
(34) Sicard, C.; Perullini, M.; Spedalieri, C.; Coradin, T.; Brayner, R.; Livage, J.; Jobbagy, M.; Bilmes, S. A. *Chem. Mater.* **2011**, *23*, 1374.
(35) Muraca, M.; Vilei, M. T.; Zanusso, G. E.; Ferraresso, C.; Boninsegna, S.; Dal Monte, R.; Carraro, P.; Carturan, G. *Artific. Organ.* **2002**, *26*, 664.
(36) Pope, E. J. A.; Braun, K.; Peterson, C. M. *J. Sol–Gel Sci. Technol.* **1997**, *8*, 635.
(37) Peterson, K. P.; Peterson, C. M.; Pope, E. J. A. *Proc. Soc. Exp. Biol. Med.* **1998**, *218*, 365.
(38) Catalano, P. N.; Bourguignon, N. S.; Alvarez, G. S.; Libertun, C.; Diaz, L. E.; Desimone, M. F.; Lux-Lantos, V. *J. Mater. Chem.* **2012**, *22*, 11681.
(39) Carturan, G.; Campostrini, R.; Dire, S.; Scardi, V.; Dealteriis, E. *J. Mol. Catal.* **1989**, *57*, L13.
(40) Premkumar, J. R.; Rosen, R.; Belkin, S.; Lev, O. *Anal. Chim. Acta* **2002**, *462*, 11.
(41) Yu, D.; Volponi, J.; Chhabra, S.; Brinker, C. J.; Mulchandani, A.; Singh, A. K. *Biosens. Bioelectron.* **2005**, *20*, 1433.

(42) Depagne, C.; Masse, S.; Link, T.; Coradin, T. *J. Mater. Chem.* **2012**, *22*, 12457.
(43) Harper, J. C.; Lopez, D. M.; Larkin, E. C.; Economides, M. K.; McIntyre, S. K.; Alam, T. M.; Tartis, M. S.; Werner-Washburne, M.; Brinker, C. J.; Brozik, S. M.; Wheeler, D. R. *Chem. Mater.* **2011**, *23*, 2555.
(44) Monton, M. R. N.; Lebert, J. M.; Little, J.; Nair, J. J.; McNulty, J.; Brennan, J. D. *Anal. Chem.* **2010**, *82*, 9365.
(45) Ge, X.; Lebert, J. M.; Monton, M. R. N.; Lautens, L. L.; Brennan, J. D. *Chem. Mater.* **2011**, *23*, 3685.
(46) Cho, E. J.; Tao, Z.; Tehan, E. C.; Bright, F. V. *Anal. Chem.* **2002**, *74*, 6177.
(47) Lee, M. Y.; Park, C. B.; Dordick, J. S.; Clark, D. S. *Proc. Natl. Acad. Sci. U.S.A.* **2005**, *102*, 983.
(48) Kiley, P.; Zhao, X. J.; Vaughn, M.; Baldo, M. A.; Bruce, B. D.; Zhang, S. G. *PLoS Biol.* **2005**, *3*, 1180.
(49) Boontheekul, T.; Kong, H. J.; Mooney, D. J. *Biomaterials* **2005**, *26*, 2455.
(50) Choi, J. K.; Lee, S. G.; Lee, J. Y.; Nam, H. Y.; Lee, W. K.; Lee, K. H.; Kim, H. J.; Lim, Y. *J. Environ. Pathol. Toxicol. Oncol.* **2005**, *24*, 163.
(51) Guzman, L. M.; Belin, D.; Carson, M. J.; Beckwith, J. *J. Bacteriol.* **1995**, *177*, 4121.
(52) Siegele, D. A.; Hu, J. C. *Proc. Natl. Acad. Sci. U.S.A.* **1997**, *94*, 8168.
(53) Pan, S. H.; Malcolm, B. A. *Biotechniques* **2000**, *29*, 1234.
(54) Nassif, N.; Roux, C.; Coradin, T.; Rager, M. N.; Bouvet, O. M. M.; Livage, J. *J. Mater. Chem.* **2003**, *13*, 203.
(55) Eleftheriou, N. M.; Ge, X.; Kolesnik, J.; Falconer, S. B.; Harris, R. J.; Khursigara, C.; Brown, E. D.; Brennan, J. D. *Chem. Mater.* **2014**, DOI: http://dx.doi.org/10.1021/cm403198z.